Soil transport driven by biological processes over millennial time scales

Joshua J. Roering* Department of Geological Sciences, University of Oregon, Eugene, Oregon 97403-1272, USA
Peter Almond, Philip Tonkin Soil, Plant, and Ecological Sciences Division, P.O. Box 84, Lincoln University, Canterbury, New Zealand
James McKean Department of Geological Sciences, University of Canterbury, Private Bag 4800, Christchurch, New Zealand

ABSTRACT

Downslope soil transport in the absence of overland flow has been attributed to numerous mechanisms, including particle-by-particle creep and disturbances associated with biological activity. Process stochasticity and difficulties associated with field measurement have obscured the characterization of relevant long-term soil transport rates and mechanisms. In a series of incised fluvial terraces along the Charwell River, South Island, New Zealand, we documented vertical profiles of tephra concentration and topographic derivatives along a hillslope transect to quantify soil transport processes. Along the undissected hilltop, we observed a thin primary tephra layer (ca. 22.6 ka) within loess deposits ~80 cm below the landscape surface. In the downslope direction, the depth to the highly concentrated tephra layer decreases, coincident with an increase in hillslope convexity (which is proportional to landscape lowering rate if soil flux varies linearly with hillslope gradient). Exhumation of the tephra layer results from landscape lowering due to disturbance-driven soil transport. Approximately 20 m downslope of the interfluve, the depth to the tephra layer declines to 40–50 cm, peak tephra concentrations decrease by a factor of 4, and tephra is distributed uniformly within the upper 40 cm of soil. The transition from a thin, highly concentrated tephra layer at depth to less concentrated, widely distributed tephra in the upper soil may result from soil mixing and transport by biological disturbances. Along our transect, the depth to this transition is ~50 cm, coincident with the rooting depth of podocarp and *Nothofagus* trees that populated the region during much of the Holocene. Our observations can be used to calibrate the linear transport model, but, more important, they suggest that over geomorphic time scales, stochastic bioturbation may generate a well-mixed and mobile soil layer, the depth of which is primarily determined by flora characteristics.

Keywords: hillslope evolution, soil transport, tephra, New Zealand, surficial processes, bioturbation.

INTRODUCTION

Soil transport on hillslopes regulates sediment delivery to channels, dictates hillslope morphology, and controls the cycling of organic material. Typically, the transport of soil in the absence of overland flow (often referred to as soil creep) is conceptualized as a slow, relatively continuous process resulting from particle-by-particle displacement (e.g., Culling, 1963). Sharpe (1938) stated that soil creep does not result from displacement along a discrete plane and can only be perceptible over long time scales. This downslope movement has been attributed to variations in soil moisture and temperature, soil water freezing, and disturbances associated with fauna and flora (Davis, 1892; Gilbert, 1909). Several soil creep theories (e.g., Kirkby, 1967) suggest that velocities should be highest near the surface and decrease gradually with depth (curve A, Fig. 1). Some studies in clay-rich soils report such convex-upward velocity profiles (e.g., Fleming and Johnson, 1975), which indicate that soil mixing should also steadily diminish with depth. In contrast, macrobiological disturbances in the upper soil column, such as root growth and tree turnover, may mix and transport soil (Schaetzl et al., 1990), such that the average particle velocity above a particular depth is relatively constant (curve B, Fig. 1). Measurement uncertainties and process stochasticity have obscured long-term patterns of soil transport and the efficacy of these two end-member models (Finlayson, 1985). In particular, annual to decadal estimates of soil velocity profiles have yielded highly variable and conflicting results, including cases where net transport was directed upslope (Clarke et al., 1999), and the dominant displacement orientation was normal to the slope (Young, 1978). Such motions seem impossible to persist over long time periods, such that their applicability to hillslope evolution remains uncertain. Unfortunately, field documentation of soil transport mechanisms and rates over geomorphically significant time scales is sparse (Heimsath et al., 2002).

Long-term characterizations of soil transport require a field methodology that documents the integrated effect of soil dynamics (Braun et al., 2001). Here we describe how primary tephra deposits can be used to quantify rates of erosion and soil transport, as well as characterize mechanisms of soil transport that have been dominant over geomorphic time scales. Our results from documenting tephra concentration profiles and topographic surveying along dissected aggradational terraces in the South Island of New Zealand illustrate for the first time that bioturbation associated with root growth and tree turnover may have outweighed other mechanisms of soil transport over the past 9 k.y. Our findings can be used for quantifying rates of erosion, transport, and soil mixing, calibrating soil transport models and simulating the development of hilly terrain.

SOIL TRANSPORT AND HILLSLOPE MORPHOLOGY

To simulate soil transport processes in numerical calculations of landscape evolution, numerous studies have represented soil transport as a slope-dependent process (e.g., Tucker and Bras, 1998). Here we use the linear, slope-dependent transport model, which is supported by field evidence (McKean et al., 1993; Small et al., 1999), to couch our field observations. This model is appropriate for low-gradient (<0.4) hillslope segments because fluxes tend to increase nonlinearly on steep slopes (Roering et al., 1999). According to the linear model, sediment flux, q_s ($m^3 \cdot m^{-1} \cdot yr^{-1}$) varies proportionally with hillslope gradient (in one dimension) as

$$q_s = -K\frac{\partial z}{\partial x}, \quad (1)$$

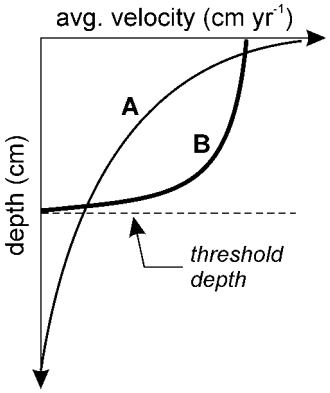

Figure 1. Schematic soil velocity profiles for particle-based soil transport models (shown by curve A) and disturbance-dominated models (shown by curve B).

*E-mail: Jroering@darkwing.uoregon.edu.

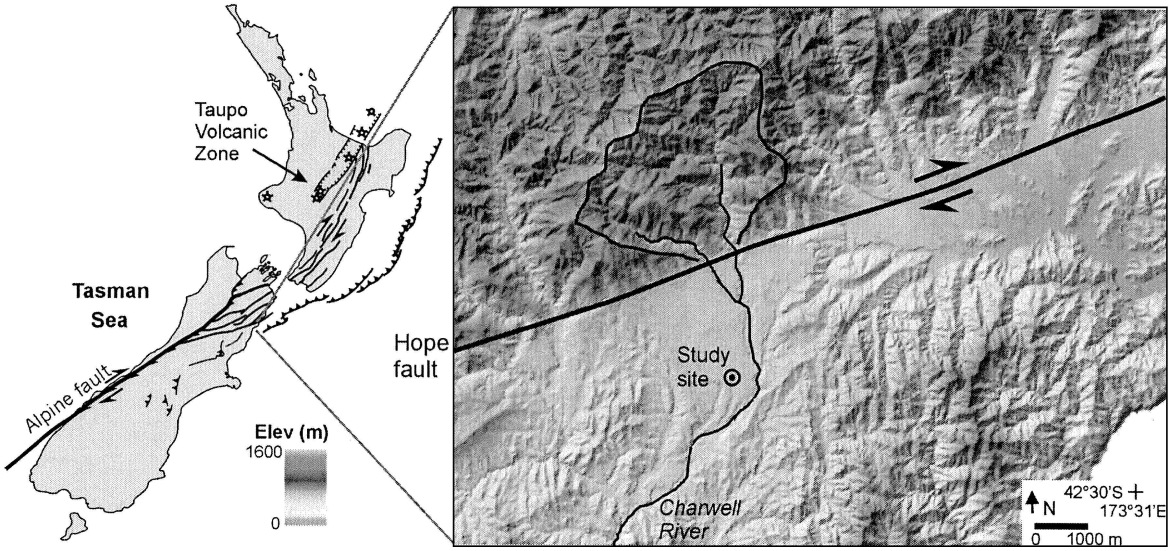

Figure 2. Location and topographic maps of Charwell River, South Island, New Zealand. Bold line defines catchment area of Charwell basin (~40 km²). Hope fault accommodates at least 20 mm·yr⁻¹ of right-lateral slip and >3 mm·yr⁻¹ of uplift.

where K is a transport rate constant ($m^2 \cdot yr^{-1}$), z is elevation (m), and x is horizontal distance (m). In this framework, soil depth does not explicitly affect the flux of sediment; instead, the depth of actively transporting soil is controlled by the mechanical action of the transport mechanisms (e.g., the depth of soil water freezing or tree rooting), assuming transport-limited conditions. The relationship between landscape lowering and sediment flux can be quantified by combining equation 1 with the one-dimensional continuity equation, yielding

$$\frac{\partial z}{\partial t} = K\frac{\partial^2 z}{\partial x^2}. \quad (2)$$

This relationship indicates that erosion is proportional to local hillslope curvature and, when coupled with topographic surveys of hillslopes, allows us to quantify spatial variability in erosion rates.

STUDY SITE: CHARWELL RIVER, SOUTH ISLAND, NEW ZEALAND

Well-documented fluvial terrace remnants of the Charwell River, South Island, New Zealand, record episodes of aggradation and channel incision through the late Quaternary (Bull, 1991). Bounding the Seaward Kaikoura Range to the north, the Hope fault separates the steep, highly dissected portion of the humid Charwell drainage basin (40 km^2) from low-relief terrain where aggradational terraces are dominant (Fig. 2). High rates of right-lateral slip (20–35 $mm \cdot yr^{-1}$) and uplift (3–6 $mm \cdot yr^{-1}$) along the Hope fault allow for the accumulation and preservation of alluvial deposits south of the range, such that terrace remnants are progressively older southwest of the current channel location (Bull, 1991). These terraces exhibit varying degrees of dissection and relief development depending on their age and position along the Hope fault. We focused the current study on hillslope development in the Dillondale terrace unit, which has been associated with the penultimate glacial advance or a previous episode of high sediment yield (Bull, 1991). This terrace unit has undergone early stages of drainage development, as flat, undissected terrace surfaces alternate with low-gradient valleys that approach 30 m in local relief.

At least three distinct loess units (totaling more than 5 m in thickness) mantle the Dillondale aggradation gravels (Fig. 3A). Detailed soil stratigraphy reveals that loess production followed (and perhaps alternated with) valley incision into the terrace gravels. Palynological data from nearby sites (W. McLea, 2001, personal commun.; McGlone and Basher, 1995) indicate that grasses dominated the area during the Last

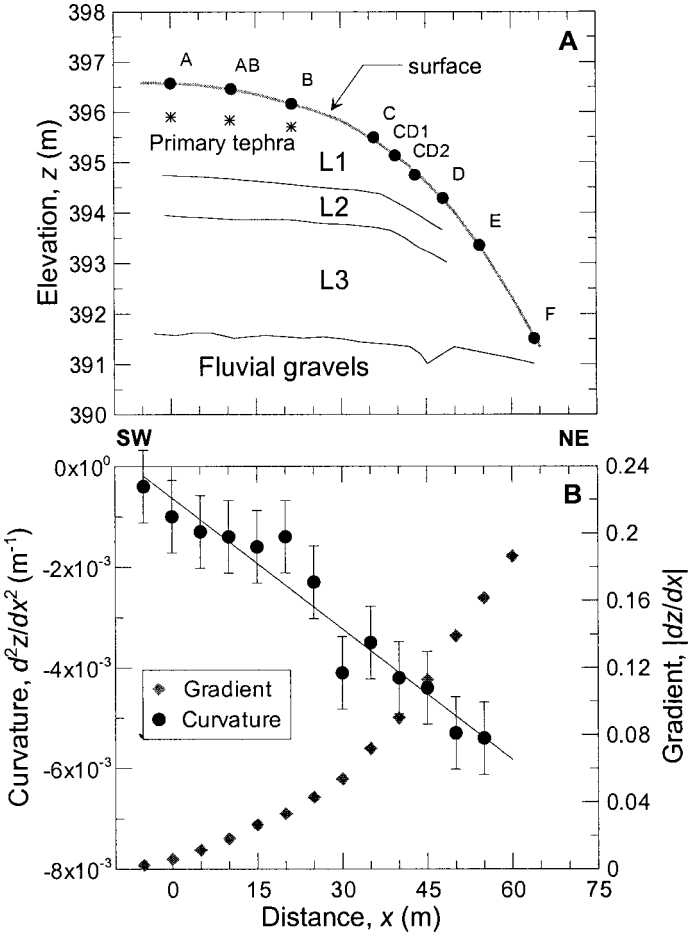

Figure 3. Morphology of study hillslope transect. A: Profile of hillslope surface elevation and soil stratigraphy. L1, L2, and L3 denote three loess units deposited on top of coarse fluvial gravels. Letters shown above surface profile denote location of continuous auger samples shown in Figure 4. B: Profiles of hillslope gradient (shown with diamonds) and hillslope curvature (shown with closed circles). Equation 2 (see text) indicates that convexity (defined here as negative curvature) is proportional to erosion rate. Error bars signify one standard error in our estimation of curvature.

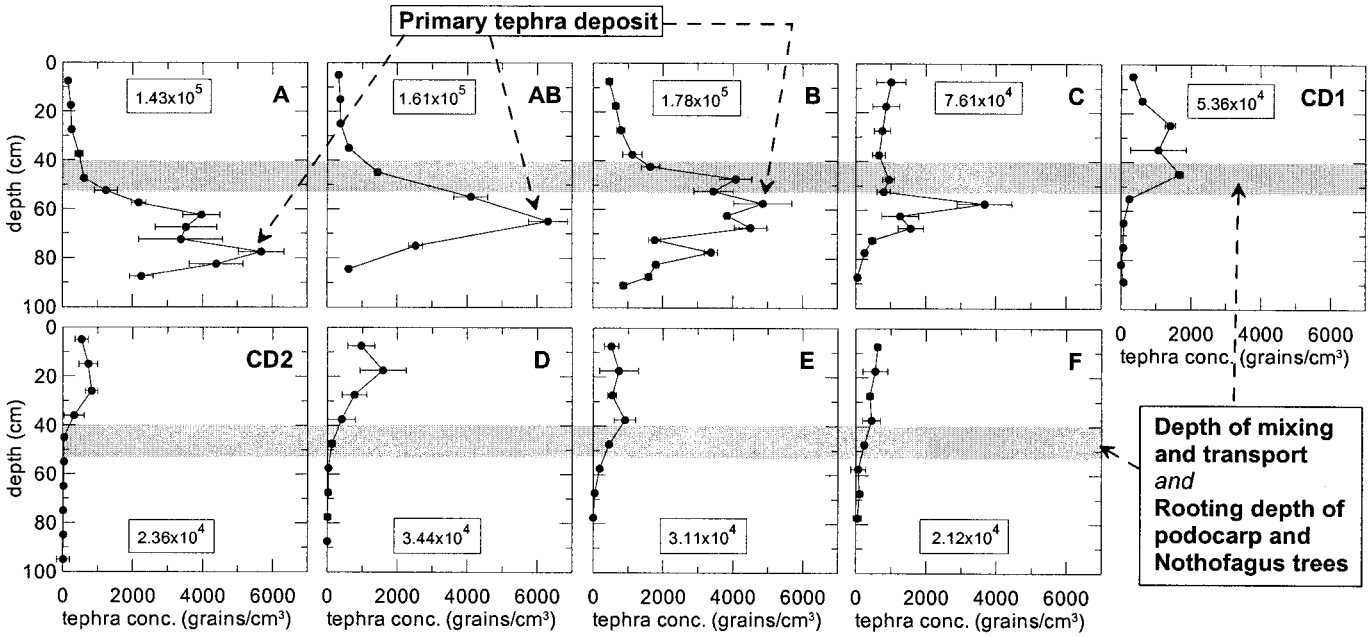

Figure 4. Depth profiles of tephra concentration for labeled sites along transect illustrated in Figure 3. Concentrations refer to tephra grains with diameters of 63–350 μm. Thick gray horizontal line denotes transition (40–55 cm) between concentrated tephra at depth and well-dispersed, low-concentration tephra in upper soil. Error bars signify one standard error in concentration estimates. Boxed number in each plot denotes depth-integrated mass of tephra (grains·cm^{-2}).

Glacial Maximum. Trees, including podocarps (*Podocarpaceae*) and beech (*Nothofagus*), became prominent following the Holocene transition and persisted until widespread burning by indigenous peoples ~700 yr ago. Primary Kawakawa tephra (22.6 ka) from the Taupo volcanic zone (see Fig. 2) occurs microscopically as glass grains within loess sheet 1, indicating that it was deposited during a period of loess production.

HILLSLOPE MORPHOLOGY AND TEPHRA CONCENTRATIONS

We documented hillslope morphology and depth profiles of tephra concentration along a 60 m hillslope transect in the Dillondale terrace to quantify erosion and sediment transport (Fig. 3A). We began the transect on an undissected, flat section of the terrace where loess thickness approaches the maximum value of 5 m. Hillslope gradient increases nonlinearly downslope, rapidly approaching 0.2 near the valley margin (Fig. 3B). Downslope of the nearly planar hilltop, hillslope convexity (defined here as negative curvature) increases linearly, coincident with a decrease in the thickness of the loess mantle. According to equation 2, erosion rates should be greatest near the valley margin and decrease upslope, attaining a minimum value atop the undissected terrace. This pattern of nonuniform erosion is consistent with valley incision and hillslope development within an initially flat surface.

Depth profiles of tephra concentration allow us to quantify exhumation (i.e., surface lowering) and the manifestation of soil mixing and transport processes. We collected vertically oriented, continuous core auger samples along the transect and determined the concentration of tephra grains in the 63–350 μm fraction using a hand-selection–based grain-counting technique. Individual tephra grains did not exhibit perceptible alteration, confirming the utility of the tephra as a conservative tracer at this site. Near the crest (site A, Fig. 4), tephra is concentrated at a depth of 80 cm and concentrations decrease rapidly toward the surface. Although the primary tephra layer was apparently buried by loess, small amounts of tephra found above the concentration peak reflect minor mixing by grasses and soil mesofauna during upbuilding of the soil profile (Almond and Tonkin, 1999). In the downslope direction (moving from site A to AB to B), the depth to the concentration peak decreases, coincident with an increase in hillslope convexity (Fig. 3B). For each of the top three auger sites (A, AB, and B), the depth-integrated mass of tephra grains is similar, suggesting that significant mass loss of tephra has not occurred (Fig. 4). Moving from site B to C the integrated mass of tephra decreases dramatically (>50%), such that the concentrated layer has been reduced to a narrow peak between 55 and 60 cm depth. Further downslope (sites CD1 through F), significant concentration peaks are not readily apparent and values in the upper 50 cm are relatively uniform. Along this lower half of the transect, concentrations below 50 cm are imperceptible, indicating that the tephra has been effectively exhumed and incorporated into the upper soil layer.

SOIL TRANSPORT MECHANISMS

If time-integrated soil velocities are highest near the surface and decrease with depth (curve A, Fig. 1), the distribution of tephra at our study site should exhibit different characteristics. According to such a model, the concentration peak would become increasingly diffuse as it approaches the surface. Instead, we observe an abrupt transition from concentrated tephra at depth to uniformly distributed tephra in the upper soil. This is particularly evident moving from site B to C, where downslope soil flux has reduced the total mass of tephra and a thin layer of high concentration remains just below the threshold depth (site C, Fig. 4). This pattern results from the combined effects of surface lowering and mixing by disturbance-driven transport processes. Bioturbation, including tree turnover and root growth (e.g., Schaetzl et al., 1990), may be the dominant mechanism responsible for detaching and displacing soil. At our study site, the depth of the transition between disturbed and undisturbed soil is consistently between 40 and 60 cm, similar to the rooting depth of *Nothofagus* and podocarp trees that colonized the area during the Holocene (W. McLea, 2001, personal commun.; McGlone and Basher, 1995; Hart et al., 2002).

Although the behavior and characteristics of individual fauna and flora may be stochastic, the integrated effect may produce a distinct signature such that soils in the active transport zone are well mixed and those below the threshold depth do not exhibit the signature of disturbance. Sites E and F provide the most compelling evidence for transport and mixing driven by disturbances. At these locations, >2 m of erosion has occurred over the past 9 k.y., and tephra grains are distributed uniformly throughout the upper 50 cm of soil. Thus, although the primary tephra layer has been exhumed and removed, re-

TABLE 1. DILLONDALE SOIL TRANSPORT CALIBRATION

Site combinations	Δz (m)	ΔC (m^{-1})	K* ($m^2 \cdot yr^{-1}$)
A-AB	0.13 ± 0.09	$9 \times 10^{-4} \pm 2 \times 10^{-4}$	0.015 ± 0.011
A-B	0.20 ± 0.011	$1.9 \times 10^{-3} \pm 2 \times 10^{-4}$	0.012 ± 0.006
AB-B	0.08 ± 0.07	$9 \times 10^{-4} \pm 1 \times 10^{-4}$	0.009 ± 0.008
mean			**0.012 ± 0.008**

*K is calculated according to equation 4, where Δt is 9 ±1 k.y.

sidual grains and grains transported from upslope are distributed evenly in the upper soil. If the soil velocity profile was convex upward (curve A, Fig. 1), any remaining tephra at sites E and F would be concentrated in the upper several centimeters because no mechanism exists to mix the tephra and distribute it evenly with depth. Our interpretations do not preclude transport by particle-based soil creep (e.g., Kirkby, 1967) at our study site; instead, stochastic disturbances associated with bioturbation may outweigh such mechanisms over geomorphic time scales.

MODEL CALIBRATION: SLOPE-DEPENDENT TRANSPORT

Combining the tephra concentration and topographic data sets enables us to calibrate the linear transport model (equation 1). We quantify differential erosion by comparing the depth of the tephra concentration peak at different locations along our transect. Assuming that the distribution of loess deposited above the tephra layer at sites A, AB, and B was relatively uniform (which is well supported by nearby observations), the magnitude of differential erosion can be calculated by subtracting modeled erosion rates at two sites along the transect using equation 2:

$$\left(\frac{\partial z}{\partial t}\right)_2 - \left(\frac{\partial z}{\partial t}\right)_1 = \mathrm{K}\left[\left(\frac{\partial^2 z}{\partial x^2}\right)_2 - \left(\frac{\partial^2 z}{\partial x^2}\right)_1\right], \quad (3)$$

where the subscripts 1 and 2 refer to two arbitrary sites along the transect. The left side of equation 3 can be approximated as $\Delta z/\Delta t$, where Δz is the difference in the depth to the tephra peak at the two sites (m), and Δt is the length of time for transport processes (yr). The right side of equation 3 can be rewritten as $\mathrm{K}\Delta C$, where ΔC is the difference in local curvature calculated at the two sites (m^{-1}). By rearranging equation 3, K is calculated as

$$\mathrm{K} = \frac{\Delta z}{\Delta C \Delta t}. \quad (4)$$

We applied equation 4 to sites where the tephra peak has not undergone significant mass loss, such that the location of the tephra peak is well delineated (i.e., combinations of sites A, AB, and B). For all of our calculations we set Δt equal to 9 ± 1 k.y., because this is the length of time with significant tree cover in our study region (McGlone and Basher, 1995). By using estimates of hillslope convexity (Fig. 3B) and depth profiles of tephra concentration (Fig. 4), we calculated the average value of K as 0.012 ± 0.008 $m^2 \cdot yr^{-1}$ (Table 1). This value is almost an order of magnitude higher than estimates of K obtained in arid environments (Hanks, 2000), although similar values were derived along forested bluffs (Nash, 1980), suggesting consistent transport rates associated with tree turnover, root growth, and associated disturbances.

DISCUSSION AND CONCLUSIONS

In this study, tephra serves as a marker bed for recording exhumation and as a tracer for documenting how transport mechanisms redistribute soil. Here we present some of the first evidence suggesting that disturbance-driven processes, such as tree uprooting and root growth, dominate soil transport over geomorphic time scales. We propose a novel methodology for calibrating the linear, slope-dependent transport model in our New Zealand study site. This calibrated value can be applied across many areas of the South Island for tasks such as morphologic dating of fault scarps, sediment-yield estimation using digital elevation data, and interpretation of differential uplift as reflected in landscape morphology.

Recent interest in the cycling of organic material in soils has spawned efforts to quantify rates of soil mixing and turnover. Our results indicate that over thousand-year time scales, soils in forested landscapes are subject to relatively uniform mixing in the upper soil. This implies that climate-related changes in flora assemblages may have significant impacts on rates of soil transport and hillslope evolution, as well as cycling of nutrients and organic material.

ACKNOWLEDGMENTS

We thank Percy Acton Adams for access to his paddocks, Bill Bull for invaluable insights and detailed background information, and Polly Hall for solid laboratory work. We commend L. Hasbargen and S. Lancaste for their thorough and insightful reviews. This research was partially funded by the Department of Geological Sciences, University of Canterbury.

REFERENCES CITED

Almond, P., and Tonkin, P., 1999, Pedogenesis by upbuilding in an extreme leaching and weathering environment, and slow loess accretion, south Westland, New Zealand: Geoderma, v. 92, p. 1–36.

Braun, J., Heimsath, A.M., and Chappell, J., 2001, Sediment transport mechanisms on soil-mantled hillslopes: Geology, v. 29, p. 683–686.

Bull, W.B., 1991, Geomorphic responses to climatic change: New York, Oxford University Press, 326 p.

Clarke, M.F., Williams, M.A.J., and Stokes, T., 1999, Soil creep: Problems raised by a 23 year study in Australia: Earth Surface Processes and Landforms, v. 24, p. 151–175.

Culling, W.E.H., 1963, Soil creep and the development of hillside slopes: Journal of Geology, v. 71, p. 127–161.

Davis, W.M., 1892, The convex profile of badland divides: Science, v. 20, p. 245.

Finlayson, B.L., 1985, Soil creep: A formidable fossil of misconception, *in* Richards, K.S., et al., eds., Geomorphology and soils: London, George Allen and Unwin, p. 141–158.

Fleming, R.W., and Johnson, A.M., 1975, Rates of seasonal creep of silty clay soil: Quarterly Journal of Engineering Geology, v. 8, p. 1–29.

Gilbert, G.K., 1909, The convexity of hilltops: Journal of Geology, v. 17, p. 344–350.

Hanks, T.C., 2000, The age of scarplike landforms from diffusion-equation analysis, *in* Noller, J.S., et al., eds., Quaternary geochronology: Methods and applications: Washington, D.C., American Geophysical Union, p. 313–338.

Hart, P.B.S., Clinton, P.W., Allen, R.B., Nordmeyer, A.H., and Evans, G., 2002, Biomass and macronutrients (above- and below-ground) in a New Zealand beech (*Nothofagus*) forest ecosystem: Implications for carbon storage and sustainable forest management: Forest Ecology and Management (in press).

Heimsath, A.M., Chappell, J., Spooner, N.A., and Questiaux, D.G., 2002, Creeping soil: Geology, v. 30, p. 111–114.

Kirkby, M.J., 1967, Measurement and theory of soil creep: Journal of Geology, v. 75, p. 359–378.

McGlone, M.S., and Basher, L.R., 1995, The deforestation of the upper Awatere catchment, Inland Kaikoura Range, Marlborough, South Island, New Zealand: New Zealand Journal of Ecology, v. 19, p. 53–66.

McKean, J.A., Dietrich, W.E., Finkel, R.C., Southon, J.R., and Caffee, M.W., 1993, Quantification of soil production and downslope creep rates from cosmogenic ^{10}Be accumulations on a hillslope profile: Geology, v. 21, p. 343–346.

Nash, D.B., 1980, Forms of bluffs degraded for different lengths of time in Emmet County, Michigan, USA: Earth Surface Processes and Landforms, v. 5, p. 331–345.

Roering, J.J., Kirchner, J.W., and Dietrich, W.E., 1999, Evidence for nonlinear, diffusive sediment transport on hillslopes and implications for landscape morphology: Water Resources Research, v. 35, p. 853–870.

Schaetzl, R.J., Burns, S.F., Small, T.W., and Johnson, D.L., 1990, Tree uprooting: Review of types and patterns of soil disturbance: Physical Geography, v. 11, p. 277–291.

Sharpe, C.F.S., 1938, Landslide and related phenomena: New York, Columbia University Press, 137 p.

Small, E.E., Anderson, R.S., and Hancock, G.S., 1999, Estimates of the rate of regolith production using ^{10}Be and ^{26}Al from an alpine hillslope: Geomorphology, v. 27, p. 131–150.

Tucker, G.E., and Bras, R.L., 1998, Hillslope processes, drainage density, and landscape morphology: Water Resources Research, v. 34, p. 2751–2764.

Young, A., 1978, A 12-year record of soil movement on a slope: Zeitschrift für Geomorphologie, supplement, v. 29, p. 104–110.

Manuscript received April 22, 2002
Revised manuscript received August 26, 2002
Manuscript accepted September 4, 2002

Printed in USA